The Plant Cell, Vol. 18, 308–320, February 2006, www.plantcell.org © 2005 American Society of Plant Biologists

Increased Expression of MAP KINASE KINASE7 Causes Deficiency in Polar Auxin Transport and Leads to Plant Architectural Abnormality in *Arabidopsis* [W]

Ya Dai,[a,1,2] Huanzhong Wang,[a,b,1] Baohua Li,[a,b] Juan Huang,[a,b] Xinfang Liu,[a] Yihua Zhou,[a] Zhonglin Mou,[a,3] and Jiayang Li[a,4]

[a] State Key Laboratory of Plant Genomics and National Center for Plant Gene Research, Institute of Genetics and Developmental Biology, Chinese Academy of Sciences, Beijing 100101, China
[b] Graduate School of the Chinese Academy of Sciences, Beijing 100101, China

Polar auxin transport (PAT) plays a crucial role in the regulation of many aspects of plant growth and development. We report the characterization of a semidominant *Arabidopsis thaliana bushy and dwarf1* (*bud1*) mutant. Molecular genetic analysis indicated that the *bud1* phenotype is a result of increased expression of *Arabidopsis MAP KINASE KINASE7* (*MKK7*), a member of plant mitogen-activated protein kinase kinase group D. We showed that BUD1/MKK7 is a functional kinase and that the kinase activity is essential for its biological functions. Compared with the wild type, the *bud1* plants develop significantly fewer lateral roots, simpler venation patterns, and a quicker and greater curvature in the gravitropism assay. In addition, the *bud1* plants have shorter hypocotyls at high temperature (29°C) under light, which is a characteristic feature of defective auxin action. Determination of tritium-labeled indole-3-acetic acid transport showed that the increased expression of *MKK7* in *bud1* or the repressed expression in *MKK7* antisense transgenic plants causes deficiency or enhancement in auxin transport, indicating that MKK7 negatively regulates PAT. This conclusion was further substantiated by genetic and phenotypic analyses of double mutants generated from crosses between *bud1* and the auxin-related mutants *axr3-3*, *tir1-1*, *doc1-1*, and *atmdr1-1*.

INTRODUCTION

The plant hormone auxin, mainly indole-3-acetic acid (IAA), plays a crucial role in a wide variety of developmental processes, including embryogenesis, apical dominance, lateral root formation, and vascular differentiation (Benkova et al., 2003; Leyser, 2003; Reinhardt et al., 2003; Morris et al., 2004). IAA is biosynthesized mainly in the shoot apex and young leaves, and its transport is quite complex both in shoots and in roots. The basipetal polar auxin transport (PAT) in shoots is important for lateral shoot inhibition because either blocking PAT or removing the shoot apex promotes shoot branching, although auxin does not enter the lateral bud directly, suggesting the existence of secondary messengers in mediating auxin action (Gil et al., 2001; Booker et al., 2003, 2004, 2005; Leyser, 2003; Sorefan et al., 2003). Auxin can also be acropetally transported into the meristem through the epidermis to induce organ formation (Reinhardt et al., 2003). In roots, IAA moves acropetally (toward the root apex) through the central vasculature and basipetally (from the root apex toward the base) through the epidermis (Muday and DeLong, 2001; Kepinski and Leyser, 2005). Inhibition of acropetal auxin transport from shoots into roots or disruption of auxin signaling significantly inhibits lateral root development (Reed et al., 1998; Casimiro et al., 2001; Rogg et al., 2001; Fukaki et al., 2002). Appropriate distribution of auxin is also necessary for normal vascular differentiation in leaves and stems. Seedlings grown in media containing auxin transport inhibitor show altered leaf vascular patterns (Galweiler et al., 1998; Mattsson et al., 1999; Steynen and Schultz, 2003), and mutations in auxin transport or signaling components confer simpler leaf venation (Hardtke and Berleth, 1998; Steynen and Schultz, 2003). In inflorescence stems, differentiation of interfascicular fibers is influenced by inhibitor treatment and altered in auxin transport mutants (Mattsson et al., 1999; Zhong and Ye, 1999).

PAT requires asymmetrically localized influx and efflux carriers on the plasma membrane (Marchant et al., 1999; Steinmann et al., 1999; Swarup et al., 2001). The permease-like AUXIN RESISTANCE1 protein, which is asymmetrically localized on the plasma membrane of root protophloem, facilitates IAA entry into cells (Marchant et al., 1999; Swarup et al., 2001). On the other hand, IAA moving out of plant cells requires efflux facilitators (Palme and Galweiler, 1999; Muday and DeLong, 2001; Friml et al., 2002). *PIN-FORMED1* (*PIN1*) encodes a membrane protein that is detectable at the basal end of auxin transport–competent

[1] These authors contributed equally to this work.
[2] Current address: Howard Hughes Medical Institute, Department of Molecular, Cell, and Developmental Biology, University of California, Santa Cruz, CA 95064.
[3] Current address: Department of Microbiology and Cell Science, University of Florida, Gainesville, FL 32611.
[4] To whom correspondence should be addressed. E-mail jyli@genetics.ac.cn; fax 8610-64873428.
The author responsible for distribution of materials integral to the findings presented in this article in accordance with the policy described in the Instructions for Authors (www.plantcell.org) is: Jiayang Li (jyli@genetics.ac.cn).
[W] Online version contains Web-only data.
Article, publication date, and citation information can be found at www.plantcell.org/cgi/doi/10.1105/tpc.105.037846.

cells in vascular tissues (Galweiler et al., 1998). Similarly, immunolocalization studies have shown that EIR1/AGR1/PIN2 that mediates gravitropism and PAT in roots is also asymmetrically localized in the carrier cells (Chen et al., 1998; Luschnig et al., 1998; Muller et al., 1998). Besides IAA influx and efflux facilitators, several other proteins identified in genetic studies in *Arabidopsis thaliana* have also been found to participate in the modulation of PAT. For example, mutation in chalcone synthase, the first enzyme in the flavonoid biosynthetic pathway, was demonstrated to enhance the auxin transport, reinforcing the conception that flavonoids may act as endogenous inhibitors in controlling auxin distribution in vivo (Brown et al., 2001; Peer et al., 2004). The *BIG* gene, encoding a calossin-like protein, was also found to play a role in auxin transport because disruption of *BIG* in the *tir3-1* (*doc1-1*) mutant displays PAT disruption phenotypes, such as decreased inflorescence height and reduced apical dominance (Gil et al., 2001). Recently, ATP binding cassette proteins were also shown to be involved in auxin transport regulation. The double mutant *atmdr1-1 atpgp1-1* was decreased in auxin transport, showing pleiotropic phenotypes such as reduced apical dominance, decreased fertility, wrinkled and curled leaves, and stunted stature (Noh et al., 2001; Luschnig, 2002). Further studies have shown that the *atmdr1-1* mutant plant displays faster and greater gravitropism (Noh et al., 2003).

Reversible protein phosphorylation may also control the activity of auxin transport proteins. The broad-spectrum kinase inhibitors staurosporine and K252a rapidly reduce auxin efflux, suggesting that protein phosphorylation may be essential to sustain the activity of the efflux carrier (Delbarre et al., 1998). Treating with auxin transport inhibitor napthylphthalamic acid (NPA) and Tyr kinase inhibitors, Bernasconi (1996) found that Tyr phosphorylation is able to reduce the regulation of auxin efflux. Genetic studies have provided further evidence that protein phosphorylation is involved in auxin transport regulation. For instance, disruption of the *RCN1* gene, which encodes the regulatory subunit of protein phosphatase 2A, leads to an increase in root basipetal auxin transport and a reduction in root gravity response (Garbers et al., 1996; Deruere et al., 1999). *PINOID*, a gene encoding a protein-Ser/Thr kinase, has been found to direct auxin transport by acting as a binary switch in apical-basal PIN polar targeting (Friml et al., 2004). Although these studies have provided useful clues, additional mutants and regulatory components are needed for a better understanding of the regulation of auxin transport.

Mitogen-activated protein kinase (MAPK) phosphorylation cascades are conserved in all eukaryotes and play essential roles in transmitting diverse stimuli, including mitogen, developmental cues, and various stress signals (Bogre et al., 2000; Ichimura, 2002; Jonak et al., 2002). A MAPK cascade consists of three classes of enzymes, MAPK, MAPK kinase (MAPKK), and MAPKK kinase (MAPKKK). MAPK is activated by dual phosphorylation of Thr and Tyr residues in a TXY motif by its upstream MAPKK, which is in turn activated by the phosphorylation of Ser and Thr residues by its upstream MAPKKK. MAPKKs with Asp at the third residue in the S/TXXXXXS/T consensus motif may also be autoactive (Kiegerl et al., 2000; Cardinale et al., 2002). Besides participating in response to various extracellular biotic and abiotic stimuli (Bogre et al., 2000; Petersen et al., 2000; Asai et al., 2002; Menke et al., 2004), MAPK cascades have been shown to be involved in developmental process and hormonal responses (Nishihama et al., 2001; Krysan et al., 2002; Lu et al., 2002; Soyano et al., 2003; Bergmann et al., 2004; Liu and Zhang, 2004).

Several lines of evidence have implicated the association of MAPK cascades with auxin action. It has been reported that extracts from 2,4-D–treated tobacco (*Nicotiana tabacum*) cells displayed a kinase activity on recombinant MPK2 protein threefold to fourfold more effective than that of the auxin-starved cells, suggesting that auxin may function as an activator of plant MAPK (Mizoguchi et al., 1994). Using an *Arabidopsis* leaf protoplast transient expression system, Kovtun and colleagues (2000) have shown that an oxidative stress MAPK cascade could negatively regulate early auxin response. In addition, auxin was shown to activate an unknown MAPK in *Arabidopsis* seedling roots (Mockaitis and Howell, 2000). However, these experiments were mainly performed in cultured cells and all lack genetic evidence. In this article, we report that *Arabidopsis MAP KINASE KINASE7* (*MKK7*) negatively regulates PAT, which in turn affects the plant architecture.

RESULTS

Isolation and Morphological Characterization of *bud1* Plants

A *bushy and dwarf 1* (*bud1*) mutant was identified from a T1 population of transgenic plants generated by a sense/antisense RNA expression system (Mou et al., 2002). In the T2 progeny, self-pollinated *bud1* plants segregated into three distinctive phenotypes, namely, severely bushy and dwarfed phenotype, an intermediate phenotype, and wild-type-like phenotype (Figures 1A, 1B, and 1E). Genetic analysis showed a segregation ratio of 95:214:84 for these three phenotypes, fitting the expected ratio of 1:2:1 ($P > 0.05$). These results suggested that the initial T1 plant was heterozygote with a semidominant mutation in a single nuclear gene, and the T2 segregants were homozygous, heterozygous, or lacking the mutation, respectively. To confirm this, T3 progeny derived from the self-pollinated wild-type-like plants and plants showing the intermediate phenotype were analyzed. As expected, all T3 progeny derived from wild-type-like T2 plants produced only wild-type plants, whereas those derived from the intermediate-phenotyped plants segregated into the three types with a ratio similar to the original T1 plant. Plants homozygous for *bud1* were highly sterile due to their shorter stamens relative to gynoecium (Figures 1C and 1D), and hand-pollination with its own pollen can restore mutant fertility.

One of the most characteristic features of the *bud1* plant is its loss of apical dominance, producing significantly more branches than the wild type at the late developmental stage (Figure 1E, Table 1). Although the *bud1* plant is strongly branched, only one lateral inflorescence emerges from each leaf axil (Figures 1B and 1E), suggesting that the extreme branching phenotype of the *bud1* plant is formed due to the continuous formation of higher order branches by releasing dormant buds from axils of rosette and cauline leaves.

The *bud1* mutant plant is significantly smaller and the inflorescence stem is more slender than the wild type (Figure 1,

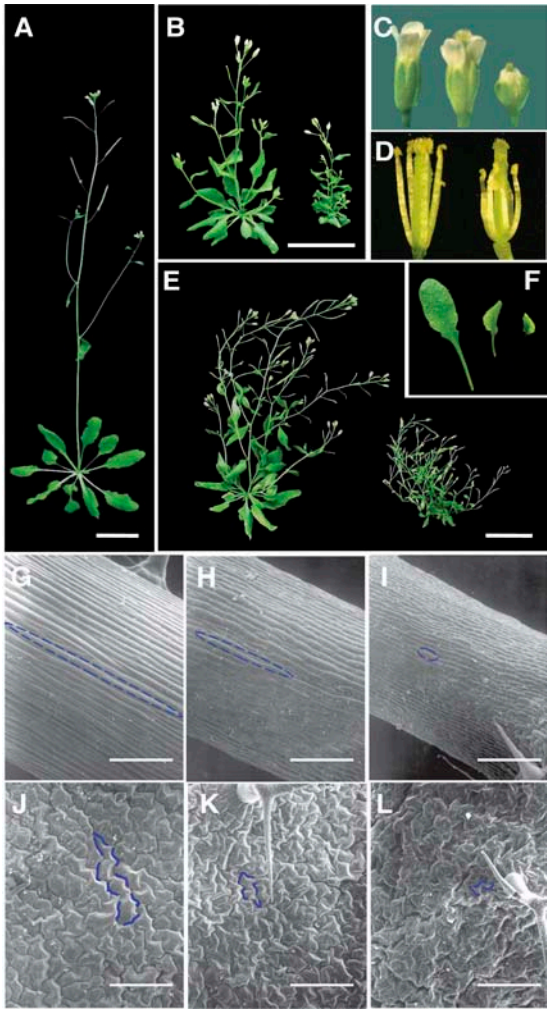

Figure 1. Morphological Comparison between Wild-Type and *bud1* Mutant Plants.

(A) The 35-d-old wild-type plant grown on soil. Bar = 2 cm.
(B) The 35-d-old *bud1* heterozygous (left) and homozygous (right) plants grown on soil. Bar = 2 cm.
(C) Flowers of wild-type (left), *bud1* heterozygous (middle) and homozygous (right) plants.
(D) Flowers of wild-type (left) and *bud1* homozygous (right) plants, showing differences in pistils and stamens.
(E) The 50-d-old *bud1* heterozygous (left) and homozygous (right) plants grown on soil. Bar = 2 cm.
(F) The third rosette leaves of wild-type (left), *bud1* heterozygous (middle), and homozygous (right) plants.
(G) to **(I)** Scanning electron microscopy of the third internodes of wild-type **(G)** and *bud1* heterozygous **(H)** and homozygous **(I)** plants. Bars = 150 μm.
(J) to **(L)** Scanning electron microscopy of the fifth rosette leaves of wild-type **(J)** and *bud1* heterozygous **(K)** and homozygous **(L)** plants. Bars = 150 μm.
Characteristic cells are marked in blue in **(G)** to **(L)**.

Table 1). When grown in soil under continuous white light, 50-d-old homozygous mutant plants are <5.0 cm in height. By contrast, the wild-type plants are taller than 24.0 cm at the same age (Table 1). The *bud1* flowers also show an altered morphology, being less elongated both in sepals and petals than those of the wild type (Figures 1C and 1D). In addition, the *bud1* petioles are shorter and the leaves are curled and smaller than those of the wild type (Figure 1F, Table 1). Scanning electron microscopic analysis further revealed defective cell expansion in *bud1* stems and leaves (Figures 1G to 1L).

Abnormalities in Hypocotyl Elongation Induced by High Temperature and Formation of Lateral Roots and Vascular System in *bud1* Plants

The loss of apical dominance and other morphological changes of *bud1* plants suggest that the mutant might be defective in auxin action. Based on the previous findings that the deficiency in auxin biosynthesis, transporting, and/or signaling would specifically affect the hypocotyl elongation induced by high temperature (Gray et al., 1998), we compared the hypocotyl elongation at high temperature between the *bud1* and wild-type plants. The hypocotyls of 9-d-old wild-type seedlings grown at 29°C were significantly longer than those at 20°C, whereas the hypocotyls of the *bud1* seedlings were slightly elongated (Figure 2A), indicating that the hypocotyl elongation at high temperature is impaired in *bud1* mutant plants.

Reduction of lateral roots has also been regarded as a criterion of the PAT disruption from shoots into roots or the disruption of auxin signaling (Reed et al., 1998; Xie et al., 2000; Rogg et al., 2001; Fukaki et al., 2002; Gray et al., 2003). As shown in Figure 2B and Table 1, 2-week-old *bud1* seedlings developed significantly less lateral roots than the wild type, suggesting that auxin polar transport or signaling may be altered in the mutant plants.

Table 1. Morphological Abnormalities of the *bud1* Plant

Measurements	*BUD1/BUD1*	*BUD1/bud1*	*bud1*
Height (cm)	23.94 ± 0.76	10.11 ± 0.41	4.09 ± 0.28
Internode length (cm)	1.56 ± 0.05	0.82 ± 0.02	0.44 ± 0.03
Leaf blade length (cm)[a]	1.44 ± 0.05	0.63 ± 0.03	0.48 ± 0.03
Leaf blade width (cm)[a]	0.67 ± 0.02	0.46 ± 0.02	0.38 ± 0.03
No. inflorescences (>5 mm)	2.63 ± 1.73	6.04 ± 0.35	10.15 ± 0.68
No. sterile siliques	0	10.50 ± 0.59	17.50 ± 1.91
No. plants measured	35	28	33
No. lateral roots per root[b]	11.88 ± 0.52	–	4.64 ± 0.46
Hypocotyl length (cm)[b]	0.57 ± 0.02	–	0.23 ± 0.01

Data shown are means ± SE. The 50-d-old plants were used for the measurement unless indicated. The differences among wild-type (*BUD1/BUD1*), heterozygous (*BUD1/bud1*), and homozygous *bud1* plants were determined with the least significant difference *t* test. All the data sets were significantly different among the three genotypes at P = 0.01.
[a] The third-paired rosette leaves.
[b] The 15-d-old seedlings grown on 0.5× MS plates were used for analysis (*n* = 30).

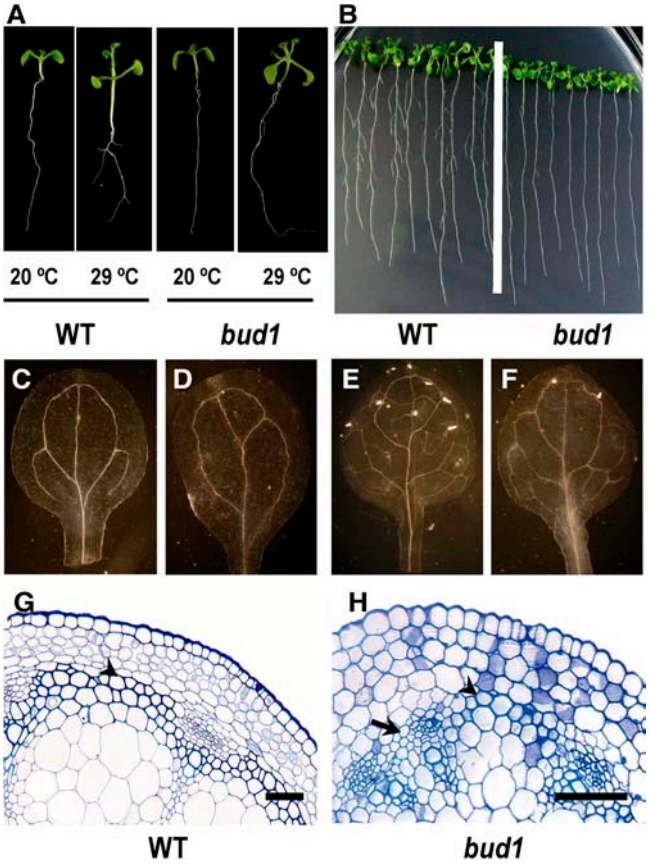

Figure 2. The *bud1* Mutant Phenotypes Seem Auxin Related.

(A) Induction of hypocotyl elongation by high temperature. Wild-type and *bud1* mutant seedlings were grown on 0.5× Murashige and Skoog (MS) plates at 20 and 29°C for 9 d and photographed with the same magnification.

(B) Comparison of lateral roots between *bud1* and wild-type plants, which were grown on 0.5× MS plates for 14 d and photographed.

(C) to **(F)** Vascular systems of cleared specimens of wild-type (**[C]** and **[E]**) and *bud1* (**[D]** and **[F]**) plants were viewed with dark-field optics. Photographs showing venation patterns of cotyledons (**[C]** and **[D]**) and leaves (**[E]** and **[F]**) of the seedlings grown on 0.5× MS plates for 12 d were taken with the same magnification.

(G) and **(H)** Microscopic comparison of the interfascicular fiber differentiation among wild-type **(G)** and homozygous *bud1* **(H)** stems, showing the presence of three layers of interfascicular fibers in the wild type and one to two layers of sclerified interfascicular cells in homozygous *bud1* (arrowhead) or no interfascicular fibers (arrow). Bars = 5 μm.

Plants exhibit characteristic vascular patterns in stems and leaves. Auxin has long been known to play a vital role in vascular patterning (Sachs, 2000; Fukuda, 2004). We therefore compared the vascular systems between wild-type and mutant plants. A simpler venation pattern was found in both cotyledon (Figures 2C and 2D) and true leaves of 12-d-old *bud1* seedlings (Figures 2E and 2F), which is similar to the venation pattern of the auxin signaling mutant *mp* or auxin transport defective mutant *pin1* (Hardtke and Berleth, 1998; Steynen and Schultz, 2003) and consistent with our previous observation that the β-glucuronidase (*GUS*) expression driven by the *DR5* promoter was altered in the leaf vascular of *bud1* mutant plants (Dai et al., 2003). Furthermore, transverse section of *bud1* mutant stems also showed less interfascicular fibers (Figures 2G and 2H).

Cloning and Molecular Characterization of *BUD1*

Genetic and molecular analysis indicated that the *bud1* mutant resulted from a single T-DNA insertion event. Genomic sequences flanking the T-DNA were recovered by screening the *bud1* genomic sublibrary using the cauliflower mosaic virus (CaMV) 35S enhancer as a probe, and the T-DNA insertion site was identified (Figures 3A and 3B). A BLASTN search of the *Arabidopsis* genomic database revealed that the T-DNA was inserted in Chromosome 1 without disrupting any known genes. However, careful analysis revealed that the T-DNA is inserted 513 bp upstream of the start codon of a putative *MKK* (*At1g18350*) and 1438 bp upstream of a putative basic transcription factor subunit (*At1g18340*) (Figure 3A). Sequence analysis of the recovered insertion locus showed that the T-DNA insertion fragment is composed of two inverted repeats, each of which contains a 2× CaMV 35S

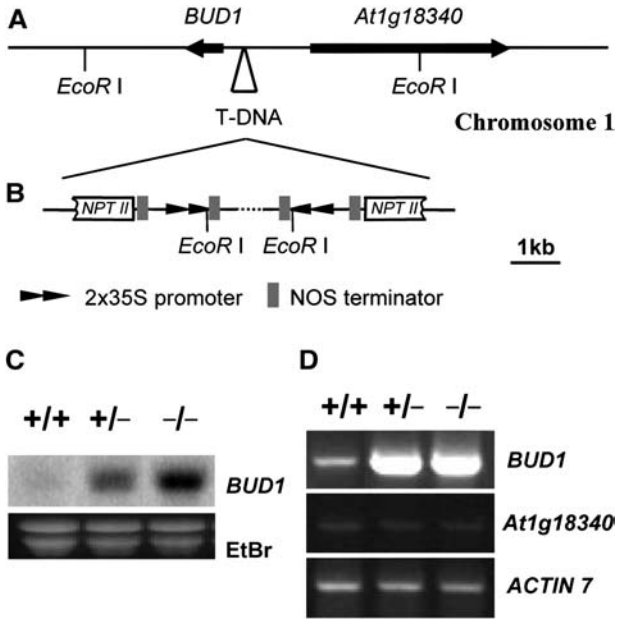

Figure 3. Cloning of *BUD1*.

(A) Physical map of the T-DNA insertion site. The T-DNA with two inverted repeats was inserted 513 bp upstream of *BUD1* and 1438 bp upstream of *At1g18340*, respectively. The arrows indicate the transcription orientations of the putative open reading frames flanking the integrated T-DNA.

(B) Structure of the integrated T-DNA in the *bud1* genome.

(C) RNA gel blot analysis of the total RNA prepared from 30-d-old soil-grown wild-type (+/+), *bud1* heterozygous (+/–), and *bud1* homozygous (–/–) plants. Ethidium bromide (EtBr)-stained total RNA was used as a loading control.

(D) RT-PCR analysis of the *BUD1* and *At1g18340* expression in 30-d-old soil-grown wild-type (+/+), *bud1* heterozygous (+/–), and *bud1* homozygous (–/–) plants. *ACTIN7* was used as an internal control.

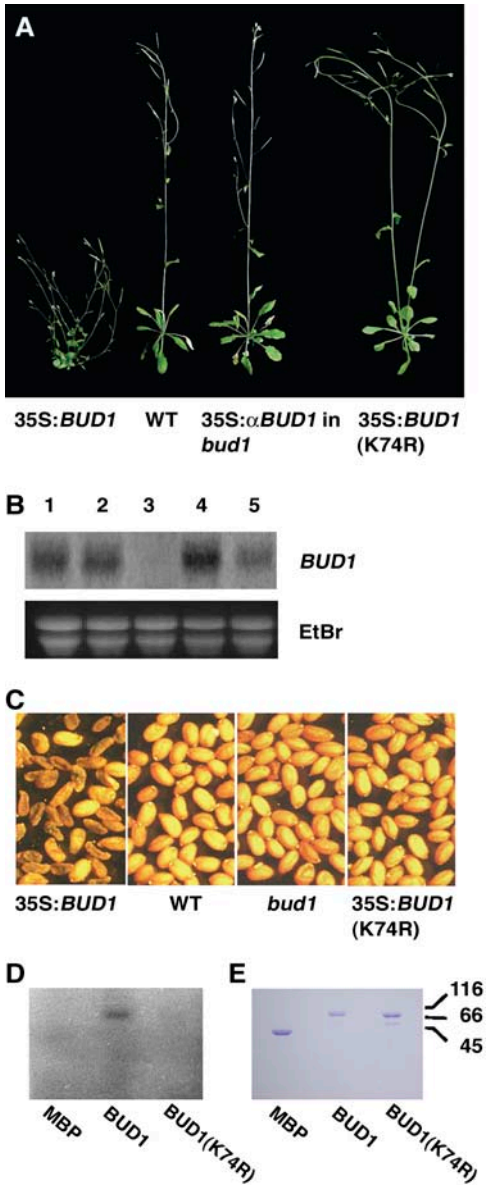

Figure 4. Confirmation and Molecular Characterization of the *BUD1* Gene.

(A) Phenotypes of transgenic plants. The transgenic plants generated from the wild-type plant transformed with the 35S:*BUD1* construct mimicked the *bud1* phenotypes but not the plant transformed with 35S:*BUD1*(K74R). The *bud1* mutant phenotype was suppressed when antisense *BUD1* (35S:α*BUD1*) construct was introduced into the *bud1* mutant plant.

(B) RNA gel blot analysis. Total RNA prepared from transgenic plants containing the 35S:*BUD1* transgene and showing the *bud1*-like phenotype (lane 1), from transgenic plants containing the 35S:*BUD1*(K74R) transgene and showing the wild-type phenotype (lane 2), from transgenic plants containing the 35S:*BUD1* transgene and showing the wild-type phenotype (lane 3), from *bud1* homozygous plants (lane 4), and from *bud1* heterozygous plants (lane 5). Ethidium bromide (EtBr)-stained total RNA was used as a loading control.

(C) T2 seeds of the *bud1*, wild-type, and transgenic plants.

(D) In vitro kinase activity assay. Autoradiogram showed the in vitro autophosphorylation of purified MBP-BUD1 or MBP-BUD1(K74R) separated by SDS-PAGE. Purified MBP was used as a negative control.

(E) Photograph of purified MBP, MBP-BUD1, and MBP-BUD1(K74R) separated by SDS-PAGE and stained with Coomassie blue.

enhancer without any cDNA insertion (Figure 3B). Surprisingly, the *NPTII* gene in the T-DNA was truncated, probably due to DNA rearrangement that might occur in the process producing the T2 generation plants because the T1 plant of *bud1* was resistant to kanamycin, but its T2 generation plants became sensitive to kanamycin. The rearrangement of the T-DNA did not affect its flanking plant DNA sequence.

The T-DNA insertion between two putative genes suggests that the mutant phenotype may result from altered expression of *At1g18340* and/or *At1g18350*. Therefore, the expression levels of both genes in the mutant and wild-type plants at the mature stage were investigated by RNA gel blot analysis. The expression level of *At1g18350* was remarkably increased in mutant plants (Figure 3C), whereas the expression of *At1g18340* was undetectable both in mutant and wild-type plants (data not shown), probably due to its extremely low expression level. We therefore employed a more sensitive method, RT-PCR, to monitor expression of these two genes. No difference of the *At1g18340* expression between mutant and wild-type plants could be found, but a dramatic increase in the *At1g18350* expression was observed (Figure 3D), as revealed by RNA gel blot hybridization. These results indicate that the *bud1* phenotype is very likely caused by an increased expression of *At1g18350*, and accordingly we designated the *At1g18350* gene as *BUD1*.

Confirmation by Transgenic Studies

To verify whether *At1g18350* represents *BUD1*, we performed two experiments. First, we placed an *At1g18350* cDNA under the control of the CaMV 35S promoter in the binary vector pBI121 and then transformed wild-type plants. Among 77 primary T1 transformants, 6 showed a *bud1*-like mutant phenotype, 56 died at different stages, and 15 were wild-type-like plants (Figure 4A). RNA gel blot analysis demonstrated that the *bud1*-like transgenic plants had an increased expression level of *BUD1*, whereas the wild-type-like transgenic plants showed no apparent increase in the *BUD1* expression level compared with that of the wild type (Figure 4B). These observations suggested that overexpression of *At1g18350* is able to recapture the *bud1* mutant phenotype. The phenotype of the surviving *bud1*-like transgenic lines includes small and curled leaves, reduced apical dominance, and reduced length and diameter of internodes (Figure 4A). Moreover, most of the seeds produced from these transgenic lines were black and shrunken (Figure 4C), lacking the ability to germinate and grow on the plates with or without supplement of kanamycin, indicating that they were embryo lethal. The seeds with normal appearance were able to geminate and grow on normal MS plates but died with supplement of kanamycin, indicating that they do not contain the transgene. These results indicated that the small number of surviving T1 transgenic lines is heterozygous for the transgene, which was

confirmed by DNA gel blot analysis (data not shown), suggesting that both homozygote and heterozygote were completely lethal in the T2 generation, probably due to the ectopic expression of *MKK7* driven by 35S promoter. Second, we overexpressed an antisense cDNA construct of *At1g18350* driven by the CaMV 35S promoter in the heterozygous *bud1* background. Out of the 23 transgenic lines, 17 displayed wild-type-like phenotype (Figure 4A), of which five lines were homozygous at the *bud1* locus (data not shown). Taken together, we conclude that *At1g18350* represents *BUD1* that is overexpressed in the *bud1* mutant plant.

BUD1 Encodes *Arabidopsis* MKK7

A *BUD1* cDNA was cloned by rapid amplification of cDNA ends (RACE)-PCR from the *bud1* total RNA by taking advantage of its overexpression feature. Sequence comparison between the *BUD1* cDNA and the genomic DNA revealed that *BUD1* contains an open reading frame of 924 bp without any intron, a 35-bp 5′ untranslated region (UTR), and a 129-bp 3′ UTR (see Supplemental Figure 1 online).

BLAST analysis suggested that *BUD1* encodes the MKK7, a member of the *Arabidopsis* MAPK cascades. In the *Arabidopsis* genome, 10 putative MAPKKs have been identified and classified into four groups (Ichimura, 2002). Phylogenetic analysis revealed that BUD1 is one of the four members in Group D, whose functions have not been identified and studied in any detail (Ichimura, 2002; Jonak et al., 2002). BUD1 contains 11 conserved kinase domains and a highly conserved motif SLDYCNS (see Supplemental Figure 1 online), in which the Ser residues are thought to be phosphorylated (Ichimura et al., 1998).

The *MKK7* expression pattern was studied using quantitative PCR. As shown in Supplemental Figure 2 online, *MKK7* was expressed in all tissues examined, with a relatively higher level in leaves and lower level in roots and flowers. In the *bud1* mutant plants, the expression pattern was similar, although the expression level was much higher. The ubiquitous expression pattern of *MKK7* was consistent with the pleiotropic mutant phenotypes.

The BUD1 Kinase Activity Is Essential for Its Biological Function

To determine whether BUD1/MKK7 has a kinase activity, we expressed and purified a maltose binding protein (MBP)-BUD1 recombinant protein from *Escherichia coli* cells. The purified MBP-BUD1 displayed an autophosphorylation activity (Figures 4D and 4E). However, no kinase activity could be detected in MBP-BUD1(K74R), in which a conserved Lys residue (K) at the position 74 of the ATP binding site in the kinase domain II was replaced with an Arg residue (R). These data indicate that MKK7 is indeed a functional kinase and its ATP binding site is indispensable.

To investigate whether the kinase activity of BUD1 is required for its biological functions in vivo, we constructed a plant transformation plasmid containing the mutated *BUD1* gene, *BUD1*(K74R), and transformed the wild-type plants. All of the 103 T1 transgenic lines containing the highly expressed *BUD1*(K74R) transgene showed the same phenotype as the wild type, whereas the transgenic plants containing the highly expressed normal *BUD1* transgene mimic the *bud1* phenotype (Figures 4A to 4C), suggesting that BUD1 kinase activity is essential for its biological activity.

Deficiency of PAT in *bud1*

Based on the finding that the *bud1* phenotype results from its deficiency in auxin action, we performed experiments to find out whether the biosynthesis, transport, and/or signaling of auxin is altered in the mutant plants. The IAA levels in 15-d-old plants grown on MS plates were measured, and no significant difference was found between the homozygous *bud1* and wild-type plants (data not shown). We then determined the sensitivity of *bud1* plants to exogenous auxin by examining the root growth inhibition by 2,4-D. As shown in Figure 5A, both *bud1* and wild-type roots showed similar sensitivity to 2,4-D, suggesting that auxin signaling in *bud1* may not be affected. Expression of two auxin-responsive genes, *IAA1* and *IAA5*, were induced to a similar degree in the roots treated with 2,4-D (Figure 5B). This is

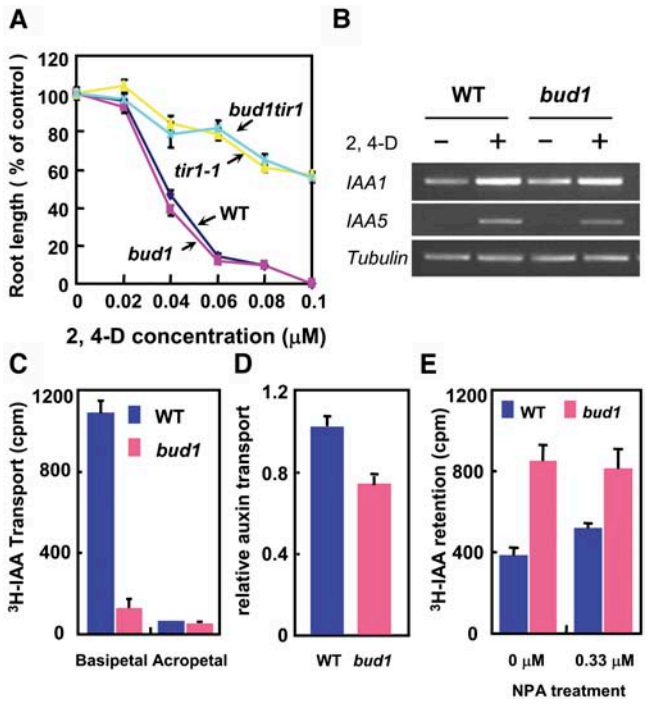

Figure 5. Auxin Transport and Gene Expression Analysis.

(A) Inhibition of root elongation by synthetic auxin 2,4-D. Each value represents the average of >10 seedlings. Bars represent ± SE.

(B) Induction of auxin-responsive genes by 2,4-D (0.04 μM) treatment in roots.

(C) PAT of inflorescence stems. Each assay used 10 wild-type and *bud1* homozygous seedlings. Values shown are means ± SE.

(D) PAT of the *bud1* and wild-type seedlings. Values are means ± SE of three independent experiments. The difference between the wild type and *bud1* is significant (Student's *t* test, $P < 0.01$).

(E) IAA efflux of dark-grown hypocotyl segments. Ten hypocotyl segments were used in each assay, and values are given as means ± SE of three to five independent assays. The difference between the wild type and *bud1* is significant (Student's *t* test, $P < 0.05$).

consistent with our previous result that the *DR5* promoter–driven *GUS* expression induced by IAA treatment was similar in *bud1* and wild-type plants (Dai et al., 2003). These results suggest that the *bud1* phenotype may result from a deficiency in PAT, rather than the auxin biosynthesis or signaling.

We therefore systematically compared the PAT between *bud1* and wild-type plants. The tritium-labeled IAA (^{3}H-IAA) basipetal transport in inflorescence stems excised from *bud1* plants was reduced to one-tenth of that in the wild type (Figure 5C), as previously reported (Dai et al., 2003). To avoid the inaccuracy resulting from the slender *bud1* inflorescence stem segments used in the assay, we further measured the auxin transport in the hypocotyl segments of both light- and dark-grown seedlings because the hypocotyl segments of *bud1* and wild-type plants are morphologically similar under these conditions. To measure basipetal movement of ^{3}H-IAA, a single microdroplet was applied to the apex of 5-d-old light-grown seedlings, and the auxin transport in the homozygous *bud1* hypocotyl segments was reduced to 72% of that of the wild type (Figure 5D). The efflux rates of auxin transport in the etiolated hypocotyls were also determined by measuring the amount of auxin retained in the hypocotyl segments after sequential incubation in the auxin-containing solution and in auxin-free buffer. As shown in Figure 5E, the ^{3}H-IAA retained in dark-grown homozygous *bud1* hypocotyls was twice as much as that of the wild type and was less sensitive to the auxin transport inhibitor NPA than that in the wild type. Taken together, all these results indicated that auxin transport in *bud1* mutant plants is deficient.

Enhanced PAT in *MKK7* Knockdown Plants

To investigate whether repressed *MKK7* expression enhances auxin transport, we generated the *BUD1* antisense transgenic lines both in the *bud1* and wild-type backgrounds. Antisense *BUD1* RNA significantly suppressed the *BUD1* expression in the *bud1* background (Figure 6A) and thereby reversed the mutant phenotype to wild type (Figures 6B and 4A) and resumed the auxin transport ability of the transgenic plant to the wild-type level (Figure 6C).

In the *BUD1* antisense transgenic plants with wild-type background, the *BUD1* expression level also decreased slightly compared with that of the wild type (Figure 6A). As the *BUD1* expression decreased, the lateral roots of antisense transgenic plants appeared 1 d earlier and more lateral roots developed (15.91 ± 0.94) than that of the wild-type plants (11.89 ± 0.52, $n = 30$, $P < 0.01$) (Figure 6B). Consistent with the concept that acropetal auxin transport in roots affects the lateral root development (Reed et al., 1998; Casimiro et al., 2001), the auxin transport from the shoot apex into the R2 segment and the root tip was significantly enhanced, although no significant enhancement in S-R TZ and R1 segments was detected (Figure 6C).

Taken together, the finding that the auxin transport was disrupted by the increased expression of *MKK7* in *bud1* and enhanced by repressed expression of *MKK7* in antisense transgenic plants suggests that MKK7 may function as a negative regulator of PAT.

Altered Gravitropism Response in *bud1* Plants

In *Arabidopsis*, PAT is required for hypocotyl elongation of light-grown seedlings but not for the dark-grown ones (Jensen et al., 1998). Consistent with this view, *bud1* showed a normal hypocotyl elongation in the dark (Figure 7A) but a shorter hypocotyl under light (Figure 2A, Table 1). We also found the absence of the apical hook of dark-grown *bud1* plants (Figure 7A), a phenotype that may be related to the auxin transport defect (Li et al., 2004; De Grauwe et al., 2005). Since the gravitropism of seedling hypocotyls is related to PAT, we further performed a gravitropism assay using etiolated seedlings. Compared with wild-type plants, the mutant hypocotyls bent to a greater degree after

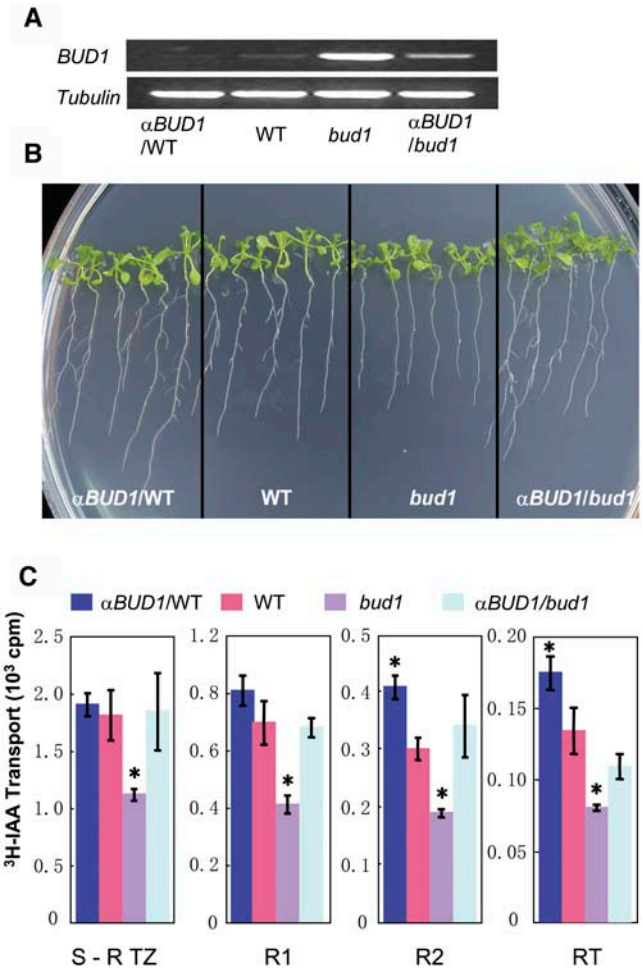

Figure 6. Analysis of the *BUD1* RNA Antisense Transgenic Plants.

(A) RT-PCR analysis of the *BUD1* expression level in the wild type, *bud1*, antisense in the wild-type background (α*BUD1*/WT), and antisense in the *bud1* background (α*BUD1*/*bud1*).

(B) Comparison of lateral roots. Plants were grown on 0.5× MS plates for 10 d and photographed.

(C) Auxin transport analysis of antisense *BUD1* transgenic lines. Auxin transport from the shoot apex to the shoot–root transition zone (S-R TZ), its subsequent two 4-mm root segments below S-R TZ (R1 and R2), and the 2- to 3-mm root tip (RT) were determined using 4.5-d-old light-grown seedlings. Ten seedlings were used in each assay. Values shown were means ± SE of five independent assays. Significance compared with the wild type (asterisks) was determined by the least significant difference *t* test at $P < 0.05$.

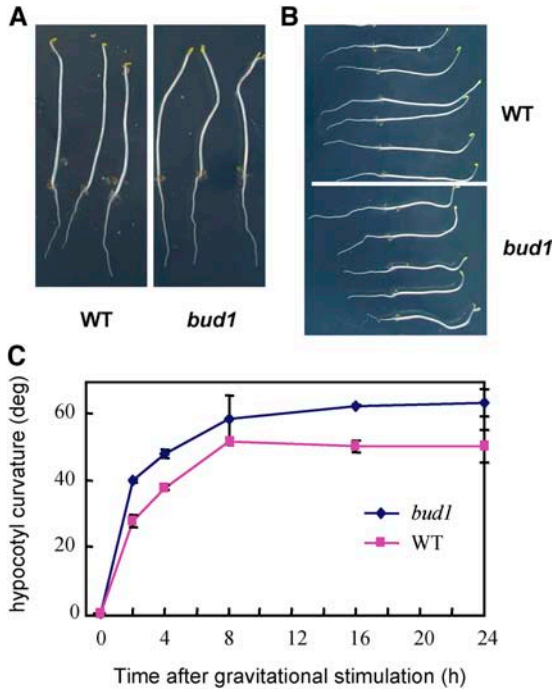

Figure 7. Comparison of Gravitropic Responses between Wild-Type and *bud1* Plants.

(A) and **(B)** Morphologies of dark-grown seedlings and their gravitropic responses. Seedlings were grown in the dark for 4 d **(A)** and then the plates were reoriented by 90° and photographed 18 h thereafter **(B)**. The *bud1* seedlings showed greater gravitropic response than the wild type. **(C)** Kinetics of hypocotyl gravitropism. Seedlings were grown in the dark for 4 d in 0.5× MS plates and reoriented by 90°. The gravitropic curvatures were measured at the time intervals as indicated. Values shown are means ± SE of five independent assays.

reorienting 90° for 18 h (Figure 7B). Kinetic analysis of the curvature development showed that the *bud1* hypocotyls bent more quickly than the wild type within the beginning 2 h after reorientation, and the bending rate tended to be the same in a prolonged period (Figure 7C). The enhanced gravitropism response of *bud1* plants was quite similar to that of *atmdr1-1*, a mutant that is defective in PAT (Noh et al., 2003).

Genetic Analyses of *bud1* Double Mutants

To further investigate the function of *BUD1*, we generated double mutants of *bud1* with either auxin-responsive or transport mutants. The auxin-resistant mutant *axr3-3* shows an enhanced apical dominance, reduced root elongation, and increased adventitious rooting and lacks root gravitropism (Leyser et al., 1996). In the *bud1 axr3-3* double mutant, the growth of axillary buds was significantly inhibited and the number of lateral branches was largely reduced compared with *bud1* mutant plants (Figures 8B to 8D), but the length of inflorescence stems was only slightly increased and the size of leaves showed no apparent alteration. This indicates that the *bud1* bushy phenotype was partially suppressed due to the hypersensitivity of *axr3-3* to auxin, suggesting that *BUD1* may act upstream of *AXR3*. Moreover, the root growth of the double mutant *bud1 tir1-1* exhibited a similar strong resistance to auxin as *tir1-1* (Figure 5A), a mutant defective in auxin signaling. These results suggested that *BUD1* may act upstream of IAA signaling.

Arabidopsis mutant *doc1-1* is involved in both auxin transport and light-related pathways and displays reduced apical dominance (Gil et al., 2001). To test whether *BUD1* functions in the same or different PAT pathways, we made a *bud1 doc1-1* double mutant and compared its phenotype with its parents. As shown in Figures 8D to 8F, the double mutant *bud1 doc1-1* exhibited an extreme dwarf phenotype, and the internode elongation between adjacent flowers was inhibited, suggesting that *BUD1* and *DOC1* might regulate auxin transport through different pathways. Since the pleiotropic phenotypes of *bud1* are strikingly similar to *atmdr1-1* and *atmdr1-1 atpgp1-1* double mutants, we further crossed *atmdr1-1* with *bud1*. The double mutant (Figure 8G) showed a very similar phenotype to *bud1* in both height and lateral branching, suggesting that they may participate in the same PAT regulatory pathway.

DISCUSSION

In *Arabidopsis*, 10 members of MAPKKs have been identified based on the annotation of the genome sequence and have been divided into four groups phylogenetically (Ichimura, 2002). Most of the members in Groups A, B, and C have been shown to play important roles in biotic and abiotic responses (Matsuoka et al., 2002; Ren et al., 2002; Teige et al., 2004). However, the function of Group D members still remains to be elucidated. In this article, we report the isolation of the *bud1* mutant and molecular genetic characterization of *MKK7*. We also present direct evidence that

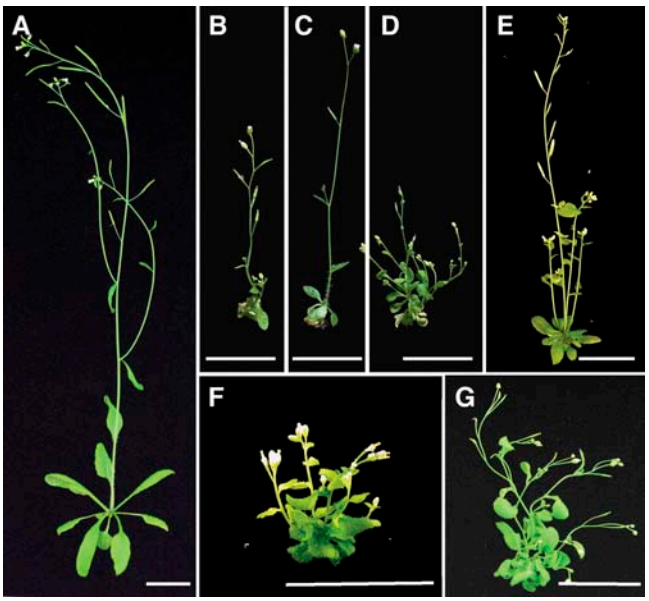

Figure 8. Phenotypes of *bud1 axr3-3*, *bud1 doc1-1*, and *bud1 atmdr1-1* Double Mutants.

Photographs were taken at 35 d after germination. **(A)** The wild type, **(B)** *axr3-3*, **(C)** *bud1 axr3-3*, **(D)** *bud1*, **(E)** *doc1-1*, **(F)** *bud1 doc1-1*, and **(G)** *bud1 atmdr1-1*. Bars = 2 cm.

the *bud1* phenotype results from the enhanced expression of *MKK7*, which negatively regulates PAT, thus affecting the formation of plant architecture.

Enhanced Expression of *MKK7* Results in Reduced Apical Dominance

Activation tagging provides an effective approach to identify genes whose expression levels play a crucial role in normal plant growth and development. The *bud1* mutant, isolated based on its abnormalities in plant architecture, may result from overexpression of *MKK7* rather than from its ectopic or constitutive expression. First, as revealed by RNA gel blot and quantitative PCR analyses, the expression of *MKK7* in *bud1* plants is strongly increased compared with the wild type, and its relative expression pattern is similar to wild-type plants. However, it may have a threshold of the *MKK7* transcripts to cause an apparent morphological phenotype because transgenic plants with weakly activated or inhibited *MKK7* showed subtle phenotypes. Overexpression of *MKK7* may result from the 2× 35S enhancer in the insertion. As previously reported, the CaMV 35S enhancer can lead to just an enhancement of the endogenous gene expression, and the phenotype resulting from such an enhancement, as opposed to true constitutive and ectopic activation, would be more likely to reflect the normal role of the activated gene (Weigel et al., 2000). Second, constitutive expression of *MKK7* in wild-type plants leads to lethality of the transgenic plants. The transgenic study of the ectopic and constitutive expression of *MKK7* driven by the CaMV 35S promoter demonstrated that most of the transgenic plants are lethal at different developmental stages, except that only a small percentage of the transgenic plants can grow like *bud1* plants but set aborted seeds. The lethality of the transgenic plants is very likely due to the ectopic and constitutive expression of *MKK7* rather than enhanced expression because RNA gel blot analysis showed that the *MKK7* expression level in the transgenic plants is much weaker than that in the *bud1* plants. Third, formation of reduced apical dominance requires the overexpression of the *MKK7* active form. Overexpression of the mutated *MKK7* form, *MKK7*(*K74R*), in which the kinase activity is abolished by a single amino acid substitution in the ATP binding site, failed to mimic the *bud1* phenotype, demonstrating that the MAPK cascade is involved in the formation of normal plant architecture of *Arabidopsis*.

Generally, the MAPKK need to be phosphorylated by its upstream MAPKKKs. However, there is a kind of MAPKK in plants that contains an Asp residue in position 3 of the consensus sequence that forms S/TXDXXXS/T located between subdomains VII and VIII. These kinds of MAPKKs, such as SALT STRESS–INDUCED MKK and other MAPKKs of the PMKK2 subfamily, may constitute an autoactive class of MAPKKs (Kiegerl et al., 2000; Cardinale et al., 2002). BUD1 falls into this kind of MAPKK. Therefore, it is possible that enhanced expression of *BUD1* could cause such a phenotype without upstream activation.

MKK7 Functions in Regulating PAT

The *bud1* morphological phenotype and its defect in the induction of hypocotyl elongation by high temperature suggest its deficiency in IAA metabolism, signaling, or transport. The findings that there are no significant differences in IAA content or in response to auxin treatment between wild-type and *bud1* plants ruled out the possibilities that IAA biosynthesis or signaling is involved in the formation of the *bud1* phenotypes. Therefore, the research focused on the auxin transport. Systematic and in-depth studies indicate that the *bud1* phenotypes result from the deficiency in polar auxin transport.

Direct evidence comes from the three different IAA transport assays, which all showed that the ^{3}H-IAA transport in *bud1* homozygous seedlings was significantly decreased. This was further strengthened by the finding that the auxin transport of *bud1* plants is less sensitive to the auxin transport inhibitor NPA than that of the wild type because of the already reduced auxin transport in the *bud1* plants. Moreover, we also showed supporting evidence that the *BUD1* expression level is consistent with the auxin transporting ability, as manifested by auxin transport and phenotypic analyses of *BUD1* antisense transgenic plants. The finding that the *BUD1* antisense transgene was more effective in *bud1* than in wild-type backgrounds may be explained by the extremely low basal expression of *BUD1* or the existence of highly homologous subgroup D genes, for example, MKK9, which is ~81% identical to BUD1.

The conclusion is also supported by the results obtained from the comparison of the hypocotyl elongation, gravitropism response, lateral root formation, lack of apical hook, and vascular patterns between the *bud1* and wild-type plants. Unlike auxin signaling mutants such as *shy2* and *axr3*, which cause photomorphogenesis in dark-grown seedlings, the dark-grown *bud1* plants showed no apparent alterations in seedling morphology or hypocotyl elongation. However, the light-grown *bud1* plants showed decreased hypocotyl elongation. This is consistent with previous studies that PAT is important for hypocotyl elongation in the light but not in the dark in *Arabidopsis* (Jensen et al., 1998). Like most PAT-deficient mutants, the *bud1* mutant also produces less lateral roots, which is a characteristic feature showing deficiency in auxin-regulated root development (Reed et al., 1998). The apical hook formation of dark-grown seedlings was controlled by interactions of auxin, ethylene, and gibberellins. Recent studies have shown that auxin and its transport may play a crucial role in this process, which is consistent with the hookless phenotype of *bud1* plants (Li et al., 2004; De Grauwe et al., 2005). Furthermore, the observation that the *bud1* plant has abnormal vascular patterns in leaves and stems could partially be explained by deficiency in auxin action, although some auxin transport inhibition phenotype was not observed (Zhong and Ye, 1999; Steynen and Schultz, 2003). This is also consistent with our previous observations that the *GUS* expression pattern guided by *DR5* promoter was altered in *bud1* mutant plants but had a similar response to exogenous auxin treatment as the wild type (Dai et al., 2003).

Genetic analysis with *bud1* double mutants also supports the conclusion that *bud1* is an auxin transport mutant resulting from enhanced expression of *MKK7*. The phenotype of the double mutant *bud1 axr3-3*, which was generated from the cross of *bud1* with auxin hypersensitive response mutant *axr3-3* (Leyser et al., 1996), is much less severe than that of *bud1* plants, indicating that the lose of apical dominance in *bud1* can be partially

suppressed by elevating its sensitivity to auxin. However, when crossed with the auxin transport decreased mutant *doc1-1* (Gil et al., 2001), the double mutant *bud1 doc1-1* showed an aggravated loss of apical dominance, which is much more severe than any parental mutant. Mutation of the *BIG* gene in *doc1-1* not only causes an auxin transport disruption phenotype but also affects the expression of light-related genes, for example, *CAB2* (Gil et al., 2001). However, the expression of *CAB2* in *bud1* plants was not affected (H. Wang, unpublished data). The extreme phenotype in *bud1 doc1-1* and the different expression patterns of *CAB2* in *bud1* and *doc1-1* plants may suggest that *MKK7* and *BIG* regulate PAT through different pathways. However, the finding that *bud1* and its double mutant *bud1 atmdr1-1* had very similar morphological phenotypes, including curled leaves, increased lateral branching, decreased plant height, and reduced fertility, may suggest the involvement of BUD1 and MDR1 in the same PAT regulatory pathway in *Arabidopsis*.

METHODS

Plant Materials and Growth Conditions

Arabidopsis thaliana ecotype Columbia (Col-0) wild-type and mutant plants were grown on vermiculite saturated with 0.3× B5 medium under continuous illumination (80 to 120 $\mu E\ m^{-2}\ s^{-1}$) at 23°C. For plants grown on 0.5× MS plates (Gibco BRL), seeds were surface sterilized. For temperature treatment, plants were germinated and grown on 0.5× MS in separate versatile environmental test chambers (Sanyo) under continuous illumination (70 $\mu E\ m^{-2}\ s^{-1}$) at 20 and 29°C, respectively. The root auxin sensitivity was assayed as follows: 4-d-old light-grown seedlings were transferred to MS plates containing appropriate concentrations of synthetic auxin 2,4-D, and the root length was measured after 3 d of treatment.

Isolation of the T-DNA–Tagged Locus

Arabidopsis genomic DNA was digested completely with *Eco*RI, separated on agarose gel, blotted onto a Hybond N^+ membrane (Amersham), and probed with CaMV 2× 35S promoter. The 7-kb DNA fragment that cosegregated with the mutant phenotype was recovered and ligated into the *Eco*RI-predigested λZAP II vector (Stratagene) to construct a sublibrary. The T-DNA–tagged locus was cloned by screening the sublibrary with 2× 35S enhancer as the probe and sequenced with a DNA Sequencer 3700 (Applied Biosystems).

RNA Gel Blot Analysis, RT-PCR, and RACE-PCR

Total RNA was prepared by a guanidine thiocyanate extraction method, and RNA gel blot analysis was performed as previously described (Hu et al., 2000). RNA (20 μg per lane) was separated in an agarose gel containing 10% formaldehyde, blotted onto a Hybond N^+ membrane (Amersham), and probed with the PCR-amplified DNA fragments using the following primers: BamHISTART (5′-GGATCCTCTCTCTTCTATTTCCATGGC-3′) and SacIEND (5′-GAGCTCACAAGCAGTCGGATCTAAAG-3′) for *BUD1/MKK7*; TFF (5′-AGGAGATGTCTTCCGCTGATG-3′) and TFR (5′-AAGTCTTCATCGGATTCGTGTG-3′) for *At1g18340*.

For RT-PCR analysis, 2 μg of total RNA treated with DNase I (Gibco BRL) was added in a 20-μL reverse transcription reaction using the Superscript first-strand synthesis system for RT-PCR (Gibco BRL), and an appropriate amount of the products was further applied for a 20-μL PCR amplification reaction using gene-specific primers, including BamHI-START and SacIEND for *BUD1/MKK7*, TFF and TFR for *At1g18340*, and ACTIN7F (5′-TGGAATGGTGAAGGCTGGTTT-3′) and ACTIN7R (5′-CTGTTGGAAGGTGCTGAGGGA-3′) for *ACTIN7*.

The 5′ and 3′ UTR sequences of *BUD1* were obtained by RACE-PCR with a 5′/3′ RACE kit (Roche). The specific primers used in RACE-PCR were SP1 (5′-GAGCTCAAGTATCATCACTCCG-3′), SP2 (5′-GCTAGTTGTTTCTCCGTAACGG-3′), SP3 (5′-CTGCTTCCTCTTCCGAGAAG-3′), and SP4 (5′-CCGTTACGGAGAAACAACTAGC-3′).

Plasmid Construction and Plant Transformation

To construct the plant transformation plasmids 35S:*BUD1* and 35S:*BUD1*(K74R) in which the Lys residue (K) at the position of 74 was point mutated into Arg (R), the DNA fragment containing the entire CDS of *BUD1* or *BUD1*(*K74R*) was double digested with *Bam*HI/*Sac*I and ligated into the pBI121 vector (Clontech). *BUD1* was amplified with primers BamHISTART and SacIEND. *BUD1*(K74R) was generated by site-directed mutagenesis PCR (Ho et al., 1989) using primer pairs of BamHISTART/BUD1muR (5′-CGTTGACTGATCTCAGAGCG-3′) and BUD1muF (5′-CGCTCTGAGATCAGTCAACG-3′)/SacIEND (the mutated base pair is underlined).

To construct 35S:antisense *BUD1* plant transformation plasmid, a 710-bp partial *BUD1* fragment truncated at the 3′ end by *Sac*I was cloned into pBI121 in an antisense orientation.

Plant transformation plasmids were introduced into *Agrobacterium tumefaciens* strain GV3101 (pMP90RK) (Koncz and Schell, 1986) by electroporation, and *Arabidopsis* plants were transformed via vacuum infiltration (Bechtold et al., 1993). Transformants (T1) were selected on plates containing 50 mg/L kanamycin and transferred to soil to allow self-pollination. Genetic and phenotypic analyses were performed mainly in T2 or T3 generations.

To generate 35S antisense *BUD1* transgenic plants in the *bud1* homozygous background, the antisense plasmid was introduced into *BUD1/bud1* heterozygous plants, and the transformants were identified by PCR analysis using the following primers: P1 (5′-TCTAGAAGCCATGGAAATAGAAGAGAG-3′), P2 (5′-CTGCAGCCGTAGGGTCATGTGTGACTG-3′), P3 (5′-ACCACGTCTTCAAAGCAAGTG-3′), and P4 (5′-TATGATAATCATCGCAAGACCG-3′).

Protein Expression and Kinase Assay

To express and purify BUD1 and BUD1(K74R) proteins for kinase assay, we amplified the coding sequences from the above-described *BUD1* and *BUD1*(*K74R*) constructs with primers BUD1EcoRIF and BUD1SalIR (5′-AGAATTCATGGCTCTTGTTCGTAAACGC-3′ and 5′-AGTCGACCTAAAGACTTTCACGGAGAAAAGG-3′). The PCR products were cloned into the *Escherichia coli* expression vector pMAL-c2 (New England Biolabs) and verified by sequencing. The fusion proteins were expressed and purified by amylose-affinity chromatography (New England Biolabs) and quantified by Bio-Rad protein assay reagent.

The autophosphorylation assay mixture (20 μL) containing 50 mM Tris-HCl, pH 7.5, 10 mM $MgCl_2$, and 10 mM $MnCl_2$, 10 μCi of γ-^{32}P-ATP, and 1 to 2 μg MBP, MBP-BUD1, or MBP-BUD1(K74R) was incubated at 30°C for 30 min, and the reaction was terminated by adding 4 μL 6× SDS-PAGE sample buffer. The reaction mixture was heated at 95°C for 5 min and then separated on a 10% (w/v) SDS-PAGE. The gel was stained with Coomassie Brilliant Blue, and the ^{32}P-labeled protein bands were visualized by the Variable Mode Imager Typhoon 8600 (Amersham Pharmacia Biotech).

Generation of *bud1* Double Mutants

The double mutant *bud1 axr3-3*, *bud1 doc1-1*, *bud1 atmdr1-1*, or *bud1 tir1-1* was generated from the cross of homozygous *bud1* with *axr3-3*, *doc1-1*, *atmdr1-1*, or *tir1-1* (Leyser et al., 1996) and identified from the F2

progeny grown on nutrient plates by comparing with its parental phenotypes and through PCR-based molecular analyses (Noh et al., 2001; Zenser et al., 2001).

IAA Measurement and Transport Assay

IAA content was measured mainly by the method described previously (Ouyang et al., 2000). Inflorescence stems of 6-week-old plants were used for auxin polar transport assay as described (Okada et al., 1991). Stem segments (2.5 cm in length) were placed in a 1.5-mL microcentrifuge tube with one end submerged in 30 μL of MES buffer (5 mM MES and 1% [w/v] sucrose, pH 5.5) containing 1.45 μM total IAA with 100 nM of ^{3}H-IAA at room temperature in darkness for 24 h. Based on the orientation of the inflorescence segment within the tube, basipetal or acropetal auxin transport was measured. After incubation, the segment was removed and the last 5 mm of the nonsubmerged end was excised and placed into 2.5 mL of scintillation fluid. The samples were allowed to sit for at least 18 h before being counted in a liquid scintillation counter.

IAA transport of dark-grown hypocotyls was assayed as described previously (Garbers et al., 1996). In each assay, 10 apical hypocotyl segments each of 2.0-mm length were put in 30 μL of transporting buffer (5 mM sodium phosphate, pH 6.0, and 1% sucrose) containing 1.0 μM IAA plus 5.0 nM ^{3}H-IAA and incubated at room temperature for 2 h with shaking at 100 rpm. The segments were washed twice and then incubated in 30 μL of buffer with shaking at 100 rpm for 2 h to allow the IAA to be transported out. After washing twice, the segments were incubated in 2.5-mL universal scintillation fluid for >18 h, and the radioactivity was counted by a liquid scintillation counter (1450 MicroBeta TriLux; Perkin-Elmer).

Auxin transport of young seedlings of wild-type and homozygous *bud1* mutant plants was assayed as previously described (Murphy et al., 2000). Plants were grown on filter paper saturated in 0.25× MS medium at 21°C for 5 d under continuous light. To assay IAA transport activity, a small drop (0.2 μL) of 10 nM ^{3}H-IAA in ethanol (50 nCi μL^{-1}) was applied onto each apical tip of 10 seedlings. After a 4-h transport period, the seedlings were rinsed with 0.25× MS medium. By removing the upper hypocotyls and cotyledons, the radioactivity in 2-mm sections excised above the transition zone was determined by a scintillation counter.

Auxin transport from shoot apex into roots was assayed using intact light-grown seedlings as described previously (Peer et al., 2004) with some modifications. Before assay, 10 seedlings grown 4.5 d after germination were transferred to vertically discontinuous filter paper strips saturated in one-quarter MS medium and allowed to equilibrate for 2 h. Auxin solutions were made up in 0.25% (w/v) agarose containing 25 mM MES, pH 5.2. A 0.2-μL microdroplet containing 500 nM unlabeled IAA and 500 nM ^{3}H-IAA (specific activity 25 Ci/mmol) was placed on the shoot apical tip of seedlings. Seedlings were then incubated in the dark for 5 h. After incubation, the hypocotyls and cotyledons were removed. A 2-mm section of filter paper, upon which the S-R TZ was centered, was harvested along with the 2-mm segment of tissue containing the S-R TZ, and the subsequent three 4-mm filter paper strip sections containing the indicated root tissue or the 2- to 3-mm root tip were also collected. The samples were allowed to sit in 2 mL of universal scintillation fluid for at least 18 h before being counted in a liquid scintillation counter.

Accession Number

Sequence data from this article can be found in the GenBank/EMBL data libraries under accession number DQ185389.

Supplemental Data

The following materials are available in the online version of this article.

Supplemental Figure 1. *BUD1* cDNA Sequence.

Supplemental Figure 2. *BUD1* Expression in Different Organs.

ACKNOWLEDGMENTS

We thank Jianru Zuo and Qi Xie (Institute of Genetics and Developmental Biology, Chinese Academy of Sciences) and reviewers for critical comments on the manuscript, Huajun Chen (Beijing Forestry University, Beijing, China) for IAA measurements, Jiayi Xie (Institute of Microbiology, Chinese Academy of Sciences) for scanning electron microscopy examination, Ottoline Leyser (University of York, UK) for providing *axr3-3* seeds, Joanne Chory (Salk Institute for Biological Studies, La Jolla, CA) for *doc1-1* seeds, and Edgar P. Spalding (University of Wisconsin, Madison, WI) for *atmdr1-1* and *atmdr1-1 atpgp1-1* seeds. This work was supported by grants from the National Natural Science Foundation of China (30221002 and 30330040) and the Ministry of Sciences and Technology of China (J02-A-001).

Received September 10, 2005; revised November 4, 2005; accepted November 18, 2005; published December 23, 2005.

REFERENCES

Asai, T., Tena, G., Plotnikova, J., Willmann, M.R., Chiu, W.L., Gomez-Gomez, L., Boller, T., Ausubel, F.M., and Sheen, J. (2002). MAP kinase signalling cascade in Arabidopsis innate immunity. Nature **415,** 977–983.

Bechtold, N., Ellis, J., and Pelletier, G. (1993). *In planta* Agrobacterium-mediated gene transfer by infiltration of *Arabidopsis thaliana* plants. C. R. Acad. Sci. (Paris) **316,** 1194–1199.

Benkova, E., Michniewicz, M., Sauer, M., Teichmann, T., Seifertova, D., Jurgens, G., and Friml, J. (2003). Local, efflux-dependent auxin gradients as a common module for plant organ formation. Cell **115,** 591–602.

Bergmann, D.C., Lukowitz, W., and Somerville, C.R. (2004). Stomatal development and pattern controlled by a MAPKK kinase. Science **304,** 1494–1497.

Bernasconi, P. (1996). Effect of synthetic and natural protein tyrosine kinase inhibitors on auxin efflux in *zucchini* (*Cucurbita pepo*) hypocotyls. Physiol. Plant **96,** 205–210.

Bogre, L., Meskiene, I., Heberle-Bors, E., and Hirt, H. (2000). Stressing the role of MAP kinases in mitogenic stimulation. Plant Mol. Biol. **43,** 705–718.

Booker, J., Auldridge, M., Wills, S., McCarty, D., Klee, H., and Leyser, O. (2004). MAX3/CCD7 is a carotenoid cleavage dioxygenase required for the synthesis of a novel plant signaling molecule. Curr. Biol. **14,** 1232–1238.

Booker, J., Chatfield, S., and Leyser, O. (2003). Auxin acts in xylem-associated or medullary cells to mediate apical dominance. Plant Cell **15,** 495–507.

Booker, J., Sieberer, T., Wright, W., Williamson, L., Willett, B., Stirnberg, P., Turnbull, C., Srinivasan, M., Goddard, P., and Leyser, O. (2005). *MAX1* encodes a cytochrome P450 family member that acts downstream of MAX3/4 to produce a carotenoid-derived branch-inhibiting hormone. Dev. Cell **8,** 443–449.

Brown, D.E., Rashotte, A.M., Murphy, A.S., Normanly, J., Tague, B.W., Peer, W.A., Taiz, L., and Muday, G.K. (2001). Flavonoids act as negative regulators of auxin transport *in vivo* in *Arabidopsis*. Plant Physiol. **126,** 524–535.

Cardinale, F., Meskiene, I., Ouaked, F., and Hirt, H. (2002). Convergence and divergence of stress-induced mitogen-activated protein kinase signaling pathways at the level of two distinct mitogen-activated protein kinase kinases. Plant Cell **14,** 703–711.

Casimiro, I., Marchant, A., Bhalerao, R.P., Beeckman, T., Dhooge, S., Swarup, R., Graham, N., Inze, D., Sandberg, G., Casero, P.J.,

and Bennett, M. (2001). Auxin transport promotes Arabidopsis lateral root initiation. Plant Cell **13,** 843–852.

Chen, R., Hilson, P., Sedbrook, J., Rosen, E., Caspar, T., and Masson, P.H. (1998). The *Arabidopsis thaliana AGRAVITROPIC 1* gene encodes a component of the polar-auxin-transport efflux carrier. Proc. Natl. Acad. Sci. USA **95,** 15112–15117.

Dai, Y., Fu, Z., and Li, J. (2003). Isolation and characterization of an Arabidopsis bush and dwarf mutant. Acta Bot. Sin. **45,** 621–625.

De Grauwe, L., Vandenbussche, F., Tietz, O., Palme, K., and Van Der Straeten, D. (2005). Auxin, ethylene and brassinosteroids: Tripartite control of growth in the Arabidopsis hypocotyl. Plant Cell Physiol. **46,** 827–836.

Delbarre, A., Muller, P., and Guern, J. (1998). Short-lived and phosphorylated proteins contribute to carrier-mediated efflux, but not to influx, of auxin in suspension-cultured tobacco cells. Plant Physiol. **116,** 833–844.

Deruere, J., Jackson, K., Garbers, C., Soll, D., and Delong, A. (1999). The *RCN1*-encoded A subunit of protein phosphatase 2A increases phosphatase activity *in vivo*. Plant J. **20,** 389–399.

Friml, J., Benkova, E., Blilou, I., Wisniewska, J., Hamann, T., Ljung, K., Woody, S., Sandberg, G., Scheres, B., Jurgens, G., and Palme, K. (2002). AtPIN4 mediates sink-driven auxin gradients and root patterning in *Arabidopsis*. Cell **108,** 661–673.

Friml, J., et al. (2004). A PINOID-dependent binary switch in apical-basal PIN polar targeting directs auxin efflux. Science **306,** 862–865.

Fukaki, H., Tameda, S., Masuda, H., and Tasaka, M. (2002). Lateral root formation is blocked by a gain-of-function mutation in the *SOLITARY-ROOT/IAA14* gene of *Arabidopsis*. Plant J. **29,** 153–168.

Fukuda, H. (2004). Signals that control plant vascular cell differentiation. Nat. Rev. Mol. Cell Biol. **5,** 379–391.

Galweiler, L., Guan, C., Muller, A., Wisman, E., Mendgen, K., Yephremov, A., and Palme, K. (1998). Regulation of polar auxin transport by AtPIN1 in Arabidopsis vascular tissue. Science **282,** 2226–2230.

Garbers, C., DeLong, A., Deruere, J., Bernasconi, P., and Soll, D. (1996). A mutation in protein phosphatase 2A regulatory subunit A affects auxin transport in *Arabidopsis*. EMBO J. **15,** 2115–2124.

Gil, P., Dewey, E., Friml, J., Zhao, Y., Snowden, K.C., Putterill, J., Palme, K., Estelle, M., and Chory, J. (2001). BIG: A calossin-like protein required for polar auxin transport in *Arabidopsis*. Genes Dev. **15,** 1985–1997.

Gray, W.M., Muskett, P.R., Chuang, H.W., and Parker, J.E. (2003). Arabidopsis SGT1b is required for SCF(TIR1)-mediated auxin response. Plant Cell **15,** 1310–1319.

Gray, W.M., Ostin, A., Sandberg, G., Romano, C.P., and Estelle, M. (1998). High temperature promotes auxin-mediated hypocotyl elongation in *Arabidopsis*. Proc. Natl. Acad. Sci. USA **95,** 7197–7202.

Hardtke, C.S., and Berleth, T. (1998). The Arabidopsis gene *MONOPTEROS* encodes a transcription factor mediating embryo axis formation and vascular development. EMBO J. **17,** 1405–1411.

Ho, S.N., Hunt, H.D., Horton, R.M., Pullen, J.K., and Pease, L.R. (1989). Site-directed mutagenesis by overlap extension using the polymerase chain reaction. Gene **77,** 51–59.

Hu, Y., Bao, F., and Li, J. (2000). Promotive effect of brassinosteroids on cell division involves a distinct CycD3-induction pathway in *Arabidopsis*. Plant J. **24,** 693–701.

Ichimura, K. (2002). Mitogen-activated protein kinase cascades in plants: A new nomenclature. Trends Plant Sci. **7,** 301–308.

Ichimura, K., Mizoguchi, T., Hayashida, N., Seki, M., and Shinozaki, K. (1998). Molecular cloning and characterization of three cDNAs encoding putative mitogen-activated protein kinase kinases (MAPKKs) in *Arabidopsis thaliana*. DNA Res. **5,** 341–348.

Jensen, P.J., Hangarter, R.P., and Estelle, M. (1998). Auxin transport is required for hypocotyl elongation in light-grown but not dark-grown *Arabidopsis*. Plant Physiol. **116,** 455–462.

Jonak, C., Okresz, L., Bogre, L., and Hirt, H. (2002). Complexity, cross talk and integration of plant MAP kinase signalling. Curr. Opin. Plant Biol. **5,** 415–424.

Kepinski, S., and Leyser, O. (2005). Plant development: Auxin in loops. Curr. Biol. **15,** R208–R210.

Kiegerl, S., Cardinale, F., Siligan, C., Gross, A., Baudouin, E., Liwosz, A., Eklof, S., Till, S., Bogre, L., Hirt, H., and Meskiene, I. (2000). SIMKK, a mitogen-activated protein kinase (MAPK) kinase, is a specific activator of the salt stress-induced MAPK, SIMK. Plant Cell **12,** 2247–2258.

Koncz, C., and Schell, J. (1986). The promoter of TL-DNA gene 5 controls the tissue-specific expression of chimeric genes carried by a novel type of *Agrobacterium* binary vector. Mol. Gen. Genet. **204,** 383–396.

Kovtun, Y., Chiu, W.L., Tena, G., and Sheen, J. (2000). Functional analysis of oxidative stress-activated mitogen-activated protein kinase cascade in plants. Proc. Natl. Acad. Sci. USA **97,** 2940–2945.

Krysan, P.J., Jester, P.J., Gottwald, J.R., and Sussman, M.R. (2002). An Arabidopsis mitogen-activated protein kinase kinase kinase gene family encodes essential positive regulators of cytokinesis. Plant Cell **14,** 1109–1120.

Leyser, H.M., Pickett, F.B., Dharmasiri, S., and Estelle, M. (1996). Mutations in the *AXR3* gene of *Arabidopsis* result in altered auxin response including ectopic expression from the *SAUR-AC1* promoter. Plant J. **10,** 403–413.

Leyser, O. (2003). Regulation of shoot branching by auxin. Trends Plant Sci. **8,** 541–545.

Li, H., Johnson, P., Stepanova, A., Alonso, J.M., and Ecker, J.R. (2004). Convergence of signaling pathways in the control of differential cell growth in *Arabidopsis*. Dev. Cell **7,** 193–204.

Liu, Y., and Zhang, S. (2004). Phosphorylation of 1-aminocyclopropane-1-carboxylic acid synthase by MPK6, a stress-responsive mitogen-activated protein kinase, induces ethylene biosynthesis in *Arabidopsis*. Plant Cell **16,** 3386–3399.

Lu, C., Han, M.H., Guevara-Garcia, A., and Fedoroff, N.V. (2002). Mitogen-activated protein kinase signaling in postgermination arrest of development by abscisic acid. Proc. Natl. Acad. Sci. USA **99,** 15812–15817.

Luschnig, C. (2002). Auxin transport: ABC proteins join the club. Trends Plant Sci. **7,** 329–332.

Luschnig, C., Gaxiola, R.A., Grisafi, P., and Fink, G.R. (1998). EIR1, a root-specific protein involved in auxin transport, is required for gravitropism in *Arabidopsis thaliana*. Genes Dev. **12,** 2175–2187.

Marchant, A., Kargul, J., May, S.T., Muller, P., Delbarre, A., Perrot-Rechenmann, C., and Bennett, M.J. (1999). AUX1 regulates root gravitropism in *Arabidopsis* by facilitating auxin uptake within root apical tissues. EMBO J. **18,** 2066–2073.

Matsuoka, D., Nanmori, T., Sato, K., Fukami, Y., Kikkawa, U., and Yasuda, T. (2002). Activation of AtMEK1, an Arabidopsis mitogen-activated protein kinase kinase, *in vitro* and *in vivo*: Analysis of active mutants expressed in *E. coli* and generation of the active form in stress response in seedlings. Plant J. **29,** 637–647.

Mattsson, J., Sung, Z.R., and Berleth, T. (1999). Responses of plant vascular systems to auxin transport inhibition. Development **126,** 2979–2991.

Menke, F.L., van Pelt, J.A., Pieterse, C.M., and Klessig, D.F. (2004). Silencing of the mitogen-activated protein kinase MPK6 compromises disease resistance in *Arabidopsis*. Plant Cell **16,** 897–907.

Mizoguchi, T., Gotoh, Y., Nishida, E., Yamaguchi-Shinozaki, K., Hayashida, N., Iwasaki, T., Kamada, H., and Shinozaki, K. (1994). Characterization of two cDNAs that encode MAP kinase homologues in *Arabidopsis thaliana* and analysis of the possible role of auxin in activating such kinase activities in cultured cells. Plant J. **5,** 111–122.

Mockaitis, K., and Howell, S.H. (2000). Auxin induces mitogenic activated protein kinase (MAPK) activation in roots of Arabidopsis seedlings. Plant J. **24,** 785–796.

Morris, A.D., Friml, J., and Zazimalova, E. (2004). Auxin transport. In Plant Hormones: Biosynthesis, Signal Transduction, Action! P.J. Davies, ed (Dordrech, The Netherlands: Kluwer Academic Publishers), pp. 437–470.

Mou, Z., Wang, X., Fu, Z., Dai, Y., Han, C., Ouyang, J., Bao, F., Hu, Y., and Li, J. (2002). Silencing of phosphoethanolamine N-methyltransferase results in temperature-sensitive male sterility and salt hypersensitivity in *Arabidopsis*. Plant Cell **14,** 2031–2043.

Muday, G.K., and DeLong, A. (2001). Polar auxin transport: Controlling where and how much. Trends Plant Sci. **6,** 535–542.

Muller, A., Guan, C., Galweiler, L., Tanzler, P., Huijser, P., Marchant, A., Parry, G., Bennett, M., Wisman, E., and Palme, K. (1998). *AtPIN2* defines a locus of *Arabidopsis* for root gravitropism control. EMBO J. **17,** 6903–6911.

Murphy, A., Peer, W.A., and Taiz, L. (2000). Regulation of auxin transport by aminopeptidases and endogenous flavonoids. Planta **211,** 315–324.

Nishihama, R., Ishikawa, M., Araki, S., Soyano, T., Asada, T., and Machida, Y. (2001). The NPK1 mitogen-activated protein kinase kinase kinase is a regulator of cell-plate formation in plant cytokinesis. Genes Dev. **15,** 352–363.

Noh, B., Bandyopadhyay, A., Peer, W.A., Spalding, E.P., and Murphy, A.S. (2003). Enhanced gravi- and phototropism in plant *mdr* mutants mislocalizing the auxin efflux protein PIN1. Nature **423,** 999–1002.

Noh, B., Murphy, A.S., and Spalding, E.P. (2001). Multidrug resistance-like genes of *Arabidopsis* required for auxin transport and auxin-mediated development. Plant Cell **13,** 2441–2454.

Okada, K., Ueda, J., Komaki, M.K., Bell, C.J., and Shimura, Y. (1991). Requirement of the auxin polar transport system in early stages of Arabidopsis floral bud formation. Plant Cell **3,** 677–684.

Ouyang, J., Shao, X., and Li, J.Y. (2000). Indole-3-glycerol phosphate, a branchpoint of indole-3-acetic acid biosynthesis from the tryptophan biosynthetic pathway in *Arabidopsis thaliana*. Plant J. **24,** 327–333.

Palme, K., and Galweiler, L. (1999). PIN-pointing the molecular basis of auxin transport. Curr. Opin. Plant Biol. **2,** 375–381.

Peer, W.A., Bandyopadhyay, A., Blakeslee, J.J., Makam, S.N., Chen, R.J., Masson, P.H., and Murphy, A.S. (2004). Variation in expression and protein localization of the PIN family of auxin efflux facilitator proteins in flavonoid mutants with altered auxin transport in *Arabidopsis thaliana*. Plant Cell **16,** 1898–1911.

Petersen, M., et al. (2000). Arabidopsis map kinase 4 negatively regulates systemic acquired resistance. Cell **103,** 1111–1120.

Reed, R.C., Brady, S.R., and Muday, G.K. (1998). Inhibition of auxin movement from the shoot into the root inhibits lateral root development in *Arabidopsis*. Plant Physiol. **118,** 1369–1378.

Reinhardt, D., Pesce, E.R., Stieger, P., Mandel, T., Baltensperger, K., Bennett, M., Traas, J., Friml, J., and Kuhlemeier, C. (2003). Regulation of phyllotaxis by polar auxin transport. Nature **426,** 255–260.

Ren, D., Yang, H., and Zhang, S. (2002). Cell death mediated by MAPK is associated with hydrogen peroxide production in *Arabidopsis*. J. Biol. Chem. **277,** 559–565.

Rogg, L.E., Lasswell, J., and Bartel, B. (2001). A gain-of-function mutation in IAA28 suppresses lateral root development. Plant Cell **13,** 465–480.

Sachs, T. (2000). Integrating cellular and organismic aspects of vascular differentiation. Plant Cell Physiol. **41,** 649–656.

Sorefan, K., Booker, J., Haurogne, K., Goussot, M., Bainbridge, K., Foo, E., Chatfield, S., Ward, S., Beveridge, C., Rameau, C., and Leyser, O. (2003). *MAX4* and *RMS1* are orthologous dioxygenase-like genes that regulate shoot branching in *Arabidopsis* and pea. Genes Dev. **17,** 1469–1474.

Soyano, T., Nishihama, R., Morikiyo, K., Ishikawa, M., and Machida, Y. (2003). NQK1/NtMEK1 is a MAPKK that acts in the NPK1 MAPKKK-mediated MAPK cascade and is required for plant cytokinesis. Genes Dev. **17,** 1055–1067.

Steinmann, T., Geldner, N., Grebe, M., Mangold, S., Jackson, C.L., Paris, S., Galweiler, L., Palme, K., and Jurgens, G. (1999). Coordinated polar localization of auxin efflux carrier PIN1 by GNOM ARF GEF. Science **286,** 316–318.

Steynen, Q.J., and Schultz, E.A. (2003). The *FORKED* genes are essential for distal vein meeting in *Arabidopsis*. Development **130,** 4695–4708.

Swarup, R., Friml, J., Marchant, A., Ljung, K., Sandberg, G., Palme, K., and Bennett, M. (2001). Localization of the auxin permease AUX1 suggests two functionally distinct hormone transport pathways operate in the Arabidopsis root apex. Genes Dev. **15,** 2648–2653.

Teige, M., Scheikl, E., Eulgem, T., Doczi, R., Ichimura, K., Shinozaki, K., Dangl, J.L., and Hirt, H. (2004). The MKK2 pathway mediates cold and salt stress signaling in *Arabidopsis*. Mol. Cell **15,** 141–152.

Weigel, D., et al. (2000). Activation tagging in *Arabidopsis*. Plant Physiol. **122,** 1003–1013.

Xie, Q., Frugis, G., Colgan, D., and Chua, N.H. (2000). Arabidopsis NAC1 transduces auxin signal downstream of TIR1 to promote lateral root development. Genes Dev. **14,** 3024–3036.

Zenser, N., Ellsmore, A., Leasure, C., and Callis, J. (2001). Auxin modulates the degradation rate of Aux/IAA proteins. Proc. Natl. Acad. Sci. USA **98,** 11795–11800.

Zhong, R., and Ye, Z.H. (1999). *IFL1*, a gene regulating interfascicular fiber differentiation in *Arabidopsis*, encodes a homeodomain-leucine zipper protein. Plant Cell **11,** 2139–2152.